



ELSEVIER

BASIC SCIENCE

Nanomedicine: Nanotechnology, Biology, and Medicine
10 (2014) 651–660



nanomedjournal.com

Original Article

Application of a hemolysis assay for analysis of complement activation by perfluorocarbon nanoparticles

Christine T.N. Pham, MD^a, Dennis G. Thomas, PhD^b, Julia Beiser, MS^c,
Lynne M. Mitchell, MS^a, Jennifer L. Huang, BS^a, Angana Senpan, PhD^d, Grace Hu, MS^c,
Mae Gordon, PhD^c, Nathan A. Baker, PhD^b, Dipanjan Pan, PhD^{d,e},
Gregory M. Lanza, MD, PhD^d, Dennis E. Hourcade, PhD^{a,*}

^aDepartment of Medicine, Division of Rheumatology, Washington University School of Medicine, St. Louis, MO, USA

^bDepartment of Knowledge, Discovery and Informatics, Pacific Northwest National Laboratory, Richland, WA, USA

^cDepartment of Ophthalmology and Visual Sciences, Division of Biostatistics, Washington University School of Medicine, St. Louis, MO, USA

^dDepartment of Medicine, Division of Cardiology, Washington University School of Medicine, St. Louis, MO, USA

^eDepartment of Bioengineering, University of Illinois at Urbana-Champaign, Champaign, IL, USA

Received 3 July 2013; accepted 29 October 2013

Abstract

Nanoparticles offer new options for medical diagnosis and therapeutics with their capacity to specifically target cells and tissues with imaging agents and/or drug payloads. The unique physical aspects of nanoparticles present new challenges for this promising technology. Studies indicate that nanoparticles often elicit moderate to severe complement activation. Using human in vitro assays that corroborated the mouse in vivo results we previously presented mechanistic studies that define the pathway and key components involved in modulating complement interactions with several gadolinium-functionalized perfluorocarbon nanoparticles (PFOB). Here we employ a modified in vitro hemolysis-based assay developed in conjunction with the mouse in vivo model to broaden our analysis to include PFOBs of varying size, charge and surface chemistry and examine the variations in nanoparticle-mediated complement activity between individuals. This approach may provide the tools for an in-depth structure-activity relationship study that will guide the eventual development of biocompatible nanoparticles.

From the Clinical Editor: Unique physical aspects of nanoparticles may lead to moderate to severe complement activation in vivo, which represents a challenge to clinical applicability. In order to guide the eventual development of biocompatible nanoparticles, this team of authors report a modified in vitro hemolysis-based assay developed in conjunction with their previously presented mouse model to enable in-depth structure-activity relationship studies.

© 2014 Elsevier Inc. All rights reserved.

Key words: Complement; Nanomedicine; Hemolysis Assay; Perfluorocarbon; Nanoparticles; Mouse Model

The project described was supported primarily by grant number U01NS073457 from the National Institutes of Health (NIH) and The Food and Drug Administration (FDA). Additional grant support from the NIH and Department of Defense (DOD) included: R01AI051436, HL112518, HL113392, CA100623, CA154737, AR056468, CA136398, Washington University Institute of Clinical and Translational Sciences grant UL1 TR000448 from the National Center for Advancing Translational Sciences (NCATS) of the NIH, and the Department of Ophthalmology and Visual Sciences at Washington University from a Research to Prevent Blindness, Inc. Unrestricted grant, and the NIH Vision Core Grant P30 EY 02687. The content is solely the responsibility of the authors and does not necessarily represent the official views of the NIH, DOD or the FDA. C.T.N.P., D.G.T., J.B., L.M.M., J.L.H., A.S., G.H., M.G., N.A.B, and D.E.H. have no commercial interests related to this work. G.M.L. is a co-inventor on a patent licensed by Washington University of St. Louis to Ocean NanoTech (ONT), Inc AR. He has co-invented patented technology licensed by Kereos, Inc from Barnes-Jewish Hospital/Washington University Medical School. He is the co-founder of Kereos, Inc, a nonexecutive CSO, has equity worth less than \$5000.00, and receives small royalty payments indirectly through the BJH-Kereos agreement. D.P. is a co-inventor on a patent licensed by Washington University of St. Louis to Ocean NanoTech (ONT), Inc AR. He serves no role, has no equity position, and receives no royalties from ONT.

We thank Dr. John Atkinson (Washington University) for helpful discussions, Mr. Nicholas Karlow and Ms. Xiaoxia Yang for technical assistance and Ms. Madonna Bogacki for help with the manuscript.

*Corresponding author at: Department of Medicine, Division of Rheumatology, Washington University School of Medicine, St. Louis, MO 63110.

E-mail address: dhourcad@dom.wustl.edu (D.E. Hourcade).

1549-9634/\$ – see front matter © 2014 Elsevier Inc. All rights reserved.

<http://dx.doi.org/10.1016/j.nano.2013.10.012>

Please cite this article as: Pham C.T.N., et al., Application of a hemolysis assay for analysis of complement activation by perfluorocarbon nanoparticles. *Nanomedicine: NBM* 2014;10:651-660, <http://dx.doi.org/10.1016/j.nano.2013.10.012>

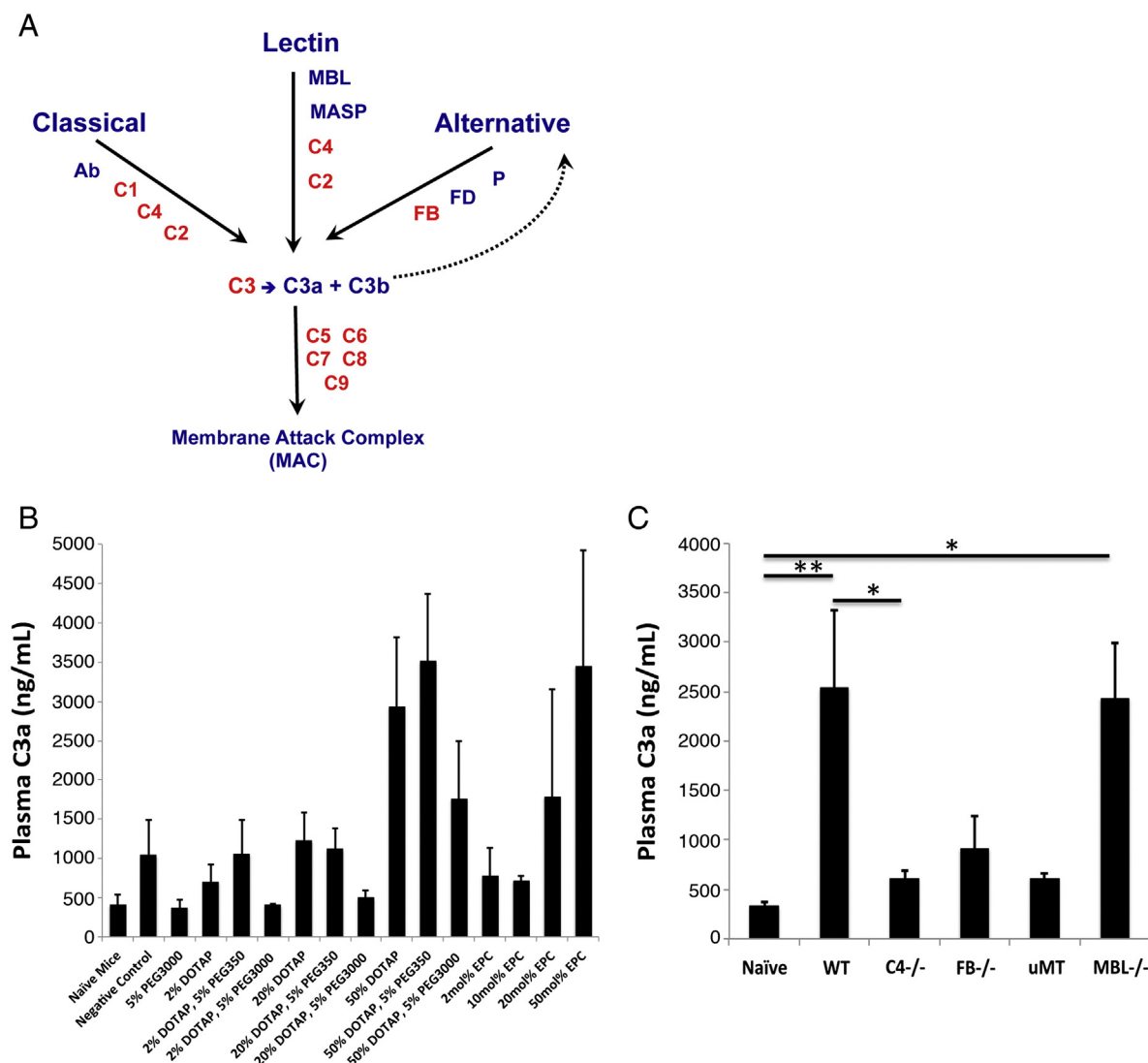


Figure 1. In vivo assay of NP-dependent C activity. **(A)** Each of the complement activation pathways (classical, lectin, and alternative) leads to the enzymatic cleavage of C3 and the formation of the membrane attack complex (MAC). Complement activity results in the consumption of the components indicated in red. **(B)** In vivo NP-dependent C activation was monitored in the mouse model system by ELISA-based quantification of plasma C3a. The data were derived from 22 naïve and 98 NP-treated animals. Each determination was performed at least 3 times except for the negative control particle ($n = 2$). **(C)** Activation of complement by the highly reactive PFOB incorporating 50 mol% DOTAP in the mouse model is dependent on antibody, C4, and factor B, but not MBL of the lectin pathway. The data were derived from $n = 3$ –12 animals per treatment group. * $P < 0.01$; ** $P < 0.001$.

Recent advances in material science have made a variety of novel therapeutic devices possible. Prominent among them are nanoparticles that can target specific cells and tissues with imaging agents and drug payloads, resulting in lower drug dosages and reduced toxicity.¹ The unique aspects of nanoparticles, however, present new challenges for this promising technology. The physical nature of nanoparticles, in comparison to that of small molecules commonly employed as drugs or contrast media, raises additional safety issues arising from interactions with cellular and other blood borne components during circulation and with the reticuloendothelial system during clearance.^{2,3} Unlike small molecules, nanoparticles are subject to the scrutiny of the immune system. In particular, the complement system is a rapid-acting, first-line host defense mechanism that defends the

intravascular space and other biological compartments from foreign invaders and cellular debris.⁴ Complement (C) recognizes potential targets, marks them for clearance and/or lysis, and initiates powerful inflammatory reactions. Some nanoparticles, such as the liposome-based therapeutic Doxil®, activate the complement system with serious clinical implications.^{5–7} While fluid phase complement regulators can mitigate limited complement activation (CA), robust activation can cause hypersensitivity (allergic) reactions and anaphylaxis, a life-threatening condition.

The three complement activation pathways lead to the cleavage of C3 to form C3b, the major complement opsonin, and C3a, an anaphylatoxin that initiates inflammatory pathways (Figure 1, A).^{4,8} The classical pathway (CP) is initiated by antibody:antigen complexes and the lectin pathway (LP) by certain polysaccharides.

The alternative pathway (AP) functions spontaneously at low level and can also serve to amplify surface activity of target-bound C3b deposited by any of the three pathways. Target-bound C3b also forms the starting point of the membrane attack complex (MAC). Host cells and tissues are protected from complement activity by cell-bound and fluid phase regulators.⁹

Perfluorocarbon nanoparticles (PFOBs) are a type of lipid-encapsulated nanoparticles that efficiently deliver imaging and therapeutic agents in several pre-clinical studies.^{10–18} In a previous report, we examined a short list of gadolinium (Gd)-functionalized PFOBs and found that several strongly activate the C system.¹⁹ Moreover, we established a close correlation between the human and mouse systems in their ability to activate C.¹⁹ Using human pooled sera depleted of specific C components and mouse strains deficient in various complement proteins^{20,21} we provided strong evidence that (Gd)-functionalized nanoparticle (NP)-mediated C activation was dependent on antibody:nanoparticle recognition and proceeded through the CP.¹⁹ These results provide the foundation for a more systematic study of structure-activity relationships of NP-dependent CA.

To further elucidate the NP:C interactions of a broader range of PFOB NPs, we began these studies using a panel of commercially available ELISAs. We were able to quantify CA *in vivo* in the mouse using ELISA-based assays, and applied them in a panel of complement-deficient mouse strains to identify the complement pathways/proteins involved in a strongly reactive PFOB. In contrast, commercial kits did not prove adequate to assess the full spectrum of PFOB-mediated CA in human sera *in vitro*. Informed by parallel *in vivo* results in mice, we modified the traditional hemolytic assay to improve sensitivity, developed a validation procedure with control particles and control reactions, and introduced a new metric to accurately quantify NP-dependent CA *in vitro*. The resulting assay was used to analyze PFOBs of varying size, charge and surface chemistry and to examine variations in NP-mediated complement activity between individuals. This approach may provide the tool for an in-depth structure-activity relationship study that will guide the eventual development of biocompatible nanoparticles.

Methods

Mice

Wild-type C57BL/6mice 6–10 weeks of age were obtained from the Jackson Laboratory (Bar Harbor, ME). WT C57BL/6, B-cell-deficient (μ MT, B6.129S2.Igh-6^{tm1Cgn}/J), and MBL-A/C^{-/-} mice (B6.129S4-Mbl1^{tm1Kata} Mbl2^{tm1Kata}/J) mice were obtained from the Jackson Laboratory, Bar Harbor, ME. C4^{-/-} and fB^{-/-} mice in C57BL/6 strain were previously described^{20,21} and generously provided by Dr. John Atkinson (Washington University). All mice were kept in a pathogen free condition at Washington University Specialized Research Facility. All the experiments were performed according to protocols approved by the Division of Comparative Medicine, Washington University School of Medicine. Under all circumstances, animals are handled with care and gentleness to minimize discomfort, distress, pain, and injury.

Complement proteins

C1 was obtained from CompTech (Tyler, TX).

Buffers

Protocols for the preparation of the following complement buffers are detailed in the Supplementary Materials.

Dextrose Veronal-buffered Saline with cations (DGVB++) (72.7 mM NaCl, 2.47 mM Na-5'-5" diethyl barbiturate, 1 mM MgCl₂, 0.15 mM CaCl₂, 2.5% (w/v) dextrose, 0.1% gelatin, pH 7.3–7.4).²²

Isotonic Veronal-buffered saline containing gelatin with cations (GVB++) (145 mM NaCl, 4.94 mM Na-5'-5" diethyl barbiturate, 1 mM MgCl₂, and 0.15 mM CaCl₂, 0.1% gelatin, pH 7.3–7.4).²²

10 mM EDTA Buffer (145 mM NaCl, 4.94 mM Na-5'-5" diethyl barbiturate, 10 mM EDTA, 0.1% gelatin, pH 7.3–7.4).²²

Antibody-sensitized sheep cells (EA)

The cells were prepared as previously described²³ with some modifications as described in the Supplementary Methods.

Human serum

Pooled human serum was purchased from CompTech (Tyler, TX), divided into aliquots (0.34 ml/aliquot, sufficient for 2 experiments without additional freeze-thaw) and stored at –80 °C until use. Pooled serum and serum derived from healthy individual donors was purchased pre-aliquoted (0.2 ml/aliquot) from Bioreclamation, LLC, and stored as above. C1s-depleted serum was obtained from CompTech.

Nanoparticles

Phospholipid-encapsulated perfluorocarbon nanoparticles (PFOBs) were prepared and characterized as described in Supplementary Materials.

Nanoparticle/serum incubation and hemolytic titration

NPs (2% v/v) were incubated in 10% pooled human serum in DGVB++ buffer (170 μ L total) for 30 min at 37 °C. Reaction mixtures were then chilled to 4 °C and cold DGVB++ buffer was added to a total of 900 μ L. For each NP reaction, a titration series was constructed consisting of 10 tubes containing ~17 μ L increments of diluted reaction mixture (V) from 0 (the buffer control) to 150 μ L, 100 μ L of EA, and DGVB++ buffer to a total of 250 μ L. Titration reactions were incubated at 37 °C for 1 h with shaking, supplemented with 665 μ L of DGVB++ buffer, and subjected to centrifugation @1800 RPM (671 rcf) at 10 °C for 5 min. Each supernatant was transferred to a 1.5 ml visible cuvette and optical density determined at 414 nm by spectrophotometry. A value for lysis control was provided in each titration series with a point consisting of 100 μ L EA mixed with water instead of buffer. The fraction of cells lysed (Y) is calculated:

$$Y = \frac{\text{OD}(\text{sample}) - \text{OD}(\text{buffer control})}{\text{OD}(100\% \text{ lysis control}) - \text{OD}(\text{buffer control})}$$

A control series was performed with serum incubated with buffer alone and the CH50 metric (the serum dilution that yields 50% lysis) was determined (Supplementary Materials). Serum control CH50 values less than 100 are indicative of poor-quality

cells. In those cases, the NP data was invalidated and cells discarded. In some other experiments the GVB++ buffer was substituted for DGVB++. Preliminary experiments were conducted at serum levels that ranged from 5–50%. The 10% serum level provided the most sensitive test of NP-dependent C activity in that range and was therefore used for the remainder of the experiments.

Quantifying the in vitro complement activity of nanoparticles

Residual Hemolytic Activity (RHA) is a measure of NP-dependent complement activity that is derived by comparing the NP titration curve to the serum control titration curve. RHA is defined as the area under the NP titration curve divided by area under the serum control titration curve. The areas under the titration curves were computed by the trapezoidal integration method. Alternatively, RHA can be simply calculated as the ratio of the sum of all values of Y for the nanoparticle-treated serum to the sum of all values of Y for the serum control.

In vivo assay of NP-dependent generation of plasma C3a and C5a

Mice at 6–12 weeks of age were injected i.v. with nanoparticles at 10 $\mu\text{L/g}$ of body weight. At this dose, 50 mol% DOTAP, used as a positive control for NP-dependent CA, consistently activated C. Blood was collected from the inferior vena cava at 30 min following NP injection directly into 10 mM EDTA tubes to prevent further ex vivo C activation. Fresh plasma was prepared from collected blood for C3a and C5a ELISA-based quantification, as previously described.¹⁷ Briefly, plates were coated overnight at 4°C with rat anti-mouse C3a (4 $\mu\text{g/mL}$) or C5a (5 $\mu\text{g/mL}$) monoclonal antibody (BD Pharmingen, San Jose, CA, USA). After being blocked with reagent diluent (1% BSA in PBS) for 1 h at RT, the plates were washed 3X with ELISA wash buffer (0.05% (v/v) Tween 20 in PBS) and incubated with samples (100 μL of same day, freshly obtained plasma diluted 1:100 in reagent diluent) for 1 h at RT. The plates were washed 3X, followed by incubation with biotinylated anti-mouse C3a (250 ng/mL) or C5a (500 ng/mL) monoclonal antibody (BD Pharmingen) for 1 h at RT. After washing, the plates were incubated with streptavidin-peroxidase (400 ng/mL; Sigma) for 30 min, washed and 100 μL of peroxide-chromogen solution (R&D Systems, Minneapolis, MN, USA) was added to each well, and color development was read at 450 nm with a SpectraMax Plus reader (Molecular Devices, Sunnyvale, CA, USA). Mouse recombinant C3a and C5a (BD Pharmingen) were used to establish the standard curve.

Statistics

Mouse C3a generation statistics

Comparisons between two groups were performed by two-tailed, unpaired t-test without correction. Comparisons between multiple groups were performed using the nonparametric Kruskal-Wallis test with post-hoc Dunn's test. P values less than 0.05 were regarded as significant.

Pooled human serum

Statistical significance of observed nanoparticle complement activity was determined by comparing residual hemolytic activity of nanoparticle-treated serum to that of serum treated with the negative control particle using the t-test (two-tailed, unequal variance). P values less than 0.05 were regarded as significant. In some cases outliers were removed before calculating the average RHA value for each nanoparticle formulation (Supplementary Table S3). The RHA values were considered as outliers if they were larger than $q_3 + w(q_3 - q_1)$ or smaller than $q_1 - w(q_3 - q_1)$, where q_1 and q_3 are the 25th and 75th percentiles, respectively, and w is 1.5.²⁴

Human serum derived from individuals

To test for the possible effect of age, race and gender on RHA of nanoparticle treated serum from individual healthy donors, we used nonparametric statistical models that are robust to departures from the normal distribution assumption. Variability in RHA among individual serum treated samples could be considerably greater than for pooled serum. Nonparametric tests included Wilcoxon 2-sample test, Kruskal-Wallis test, and Spearman rank order correlation implemented with SAS (V9.3). For analytic purposes, the results from 2 to 3 experiments were averaged for each of 24 individuals. Because these pilot studies using individual human serum were exploratory, we adopted a more lenient threshold for 'statistical significance' of at 0.10 or less, to decrease the probability of missing an important potential effect.

Results

Quantitative analysis of NP-dependent C activity in the mouse in vivo model

The mouse provides a well-characterized in vivo model for C activation/regulation that has been employed in numerous complement-dependent disease and injury studies {reviewed in²⁵ and²⁶}. Our previous studies revealed striking similarities between the in vivo mouse C and in vitro human C responses to the negatively-charged PFOB nanoparticles that harbor surface Gd-based imaging agents,¹⁹ demonstrating the added strength of a combined in vitro and in vivo approach to understanding the mechanism of NP-dependent CA. To quantitatively assess in vivo C activation in a broader range of PFOBs, we turned to ELISA-based quantification of plasma C3a and C5a, products of all three complement activation pathways (Figure 1, A). When examining a panel of positively-charged PFOBs we detected more CA with increasing surface load of N-[1-(2,3-Dioleoyloxy)propyl]-N,N,N-trimethylammonium methyl-sulfate (DOTAP) or 1,2-dioleoyl-*sn*-glycero-3-ethylphosphocholine (EPC) surface load (Figure 1, B). The incorporation of PEG3000, but not PEG350, significantly diminished CA by 2 mol% and 20 mol% DOTAP particles ($P < 0.02$, Figure 1, B). Of note, we did not detect in vivo C5a accumulation above that observed with control particles or in naïve mice, even with 50 mol% DOTAP, the strongest C activating NP (data not shown). Additional analysis with 50 mol% DOTAP particles was undertaken with a panel of mice deficient in specific complement components

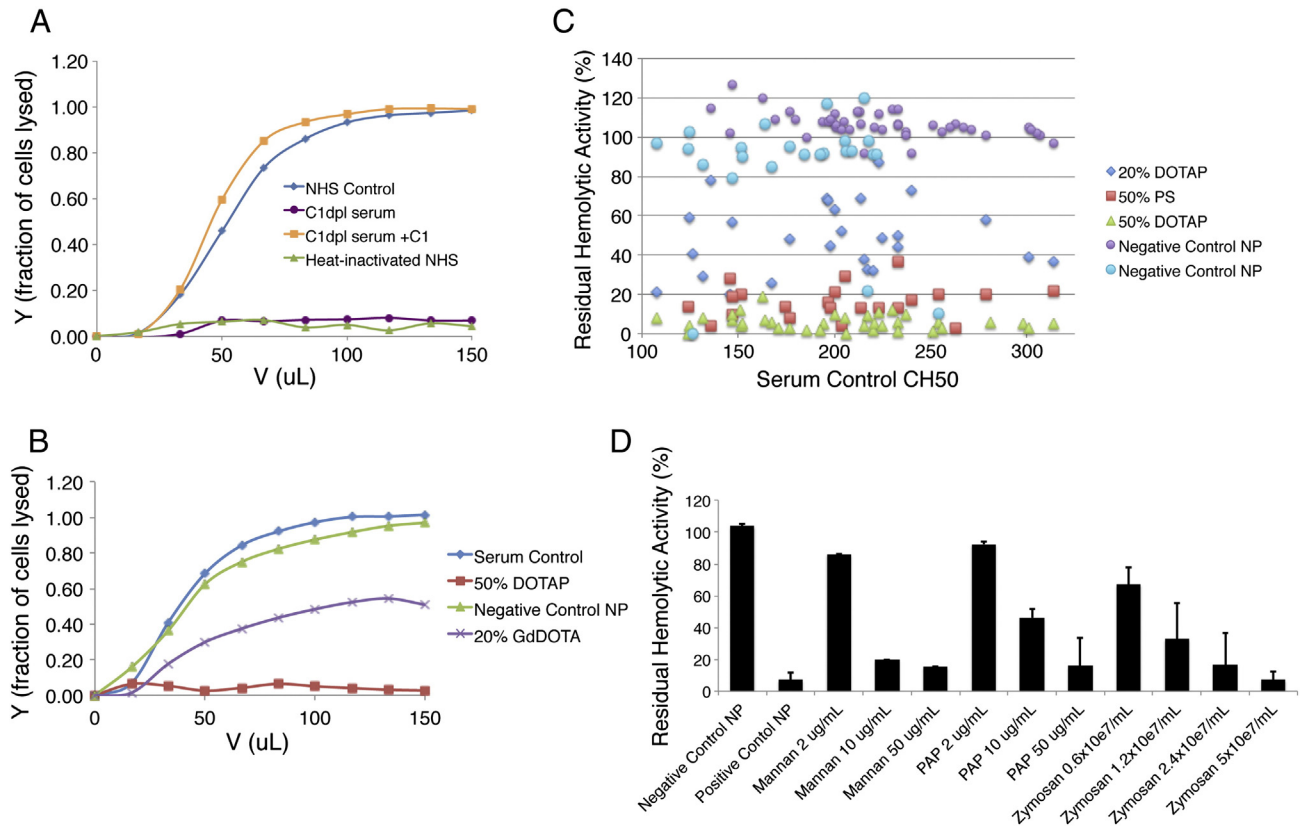


Figure 2. Hemolysis assay of nanoparticle-dependent complement activation. **(A)** Each curve in a titration series is derived by plotting the volume of reaction mixture (V) in each titration point on the x-axis versus the fraction of EA lysed (Y) on the y-axis. The serum control titration curve reaches a plateau at complete cell lysis ($Y = 1$). Hemolysis requires the presence of the CP protein C1 and is inhibited by heat-inactivation of serum complement components. **(B)** Incubation with a strong C-activating NP (50 mol% DOTAP) leads to complete loss of serum complement components that is reflected by diminished hemolytic activity and a downward shift of the titration curve. Incubation with a negative control NP results in no C activation and a titration curve that is nearly superimposed on the serum control curve. Moderate C activation (with 20 mol% GdDOTA) results in an intermediate curve **(C)** Nanoparticle:C activity, assessed as residual hemolytic activity, is relatively constant over a broad range of CH50 values. **(D)** Dose-dependent depletion of hemolytic activity by standard the complement activators mannan, peroxidase/antiperoxidase complexes (PAP) and zymosan.

(Figure 1, C). The absence of CP protein C4 greatly attenuated while the absence of the AP protein factor B moderately diminished C3 production, providing strong evidence that both of these pathways were activated by the nanoparticle. In addition, NP-dependent C3a production was not detected in the μ MT mouse strain, in which animals lack the capacity to produce antibodies. Together these results indicate that, in the wild type mouse, antibody-dependent recognition of the NP triggers CP activation, which is amplified by the AP. While the LP can in some cases be initiated by antibody:antigen complexes^{27,28} and can also operate in the absence of C4,²⁸ we found that C3a generation did not appear to be altered in mice deficient in the LP recognition proteins MBL-A/C (Figure 1, C), suggesting that the LP was not involved.

Hemolytic assay of nanoparticle:complement activity

To correlate the in vivo results with in vitro NP-dependent C activity using human sera, we turned to a panel of commercially available ELISA-based assays. Several investigations have used these assays to evaluate C activity of several nanoparticle types.^{29–32}

Each ELISA measures the generation of a single complement activation product (C3a, C4d, C5a, SC5b-9). We employed the ELISAs to quantify in vitro NP-dependent C activity but the inherent high background and/or low sensitivity we encountered confounded our efforts (Supplementary Materials and Supplementary Figures S1–S5). We next turned to an alternative methodology, a hemolysis-based assay. In the clinical setting, the hemolysis assay has been used for decades to quantify total C activity of human serum by defining the CH50, the serum dilution that results in 50% lysis of antibody-sensitized sheep red blood cells, and to quantify AP-specific activity by defining the APCH50.²² It can also be employed to assess NP-dependent C activity.^{19,33}

To perform the hemolysis assay, nanoparticles were first pre-incubated with pooled human serum. During this incubation, NP-dependent C activation via any of the three complement pathways will cause irreversible loss (depletion) of several C components (Figure 1, A). The reaction mixture is then titrated to determine its residual C activity: incremental increases of the reaction mixture were added to a fixed volume of antibody-sensitized sheep cells (EA) and allowed a second incubation, during which time the sensitized EA cells are subject to lysis by residual C components in

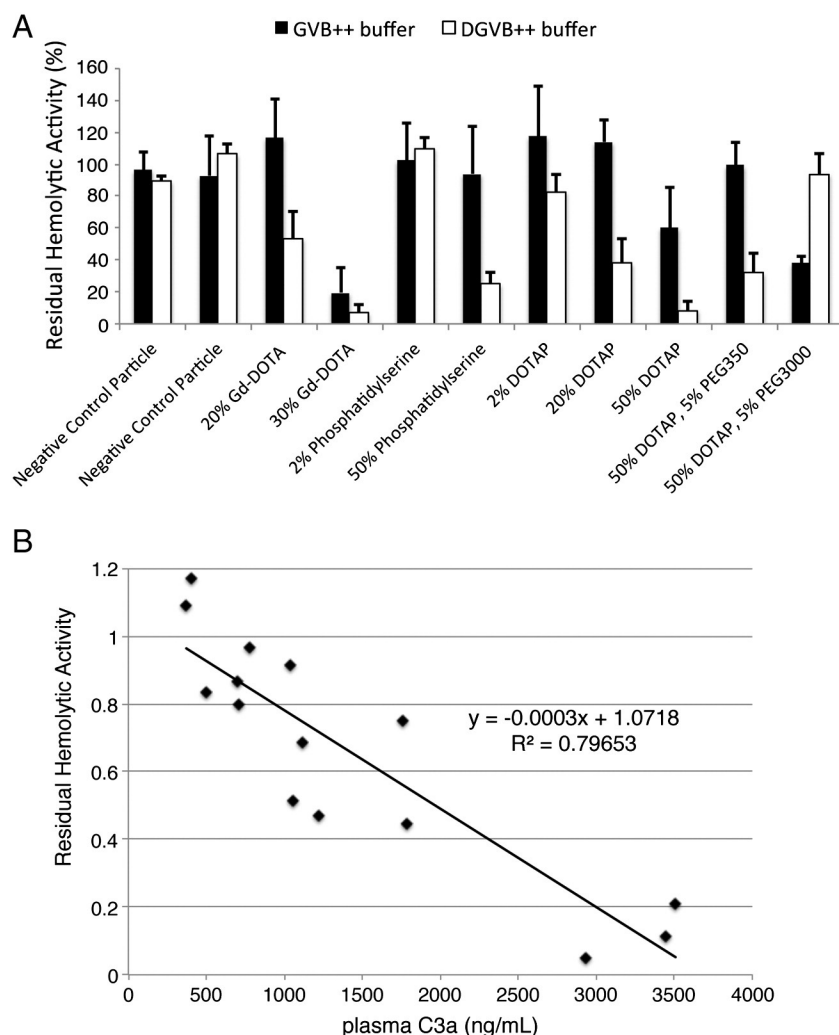


Figure 3. Correlation of the hemolysis assay to the animal model. **(A)** Sensitivity of the hemolysis assay is enhanced with low ionic strength DGVB⁺⁺ buffer vs physiological ionic strength buffer (GVB⁺⁺). The data was derived from 18 pairs of experiments (see Supplementary Methods). Each NP was assayed at least 5 times in each buffer. **(B)** In vivo NP-dependent plasma C3a production (Figure 2, A) compared to in vitro CA as measured with DGVB⁺⁺ buffer (see also Supplemental Table 2). Trendline was derived by linear regression analysis ($R^2 = 0.80$). The data points also fitted a logarithmic regression with $R^2 = 0.83$.

the human serum. Lysis in this assay is CP-dependent and requires the functional assembly of the MAC.^{4,8} Each titration series can be represented graphically as a curve with the volume of reaction mixture (V) in each titration point on the x-axis versus the fraction of EA lysed (Y) on the y-axis (Figure 2, A). Incubation with negative control NPs results in no detectable C activation and a titration curve that is superimposed on the serum control curve. Incubation with C-activating NPs leads to depletion of C activity in the serum, which is reflected in diminished lytic activity and a shift of the titration curve (Figure 2, B).

To quantify NP-dependent CA we compared the area under the nanoparticle titration curve (AUC_{NP}) to that of the serum control titration curve (AUC_{SC}). That ratio (AUC_{NP}/AUC_{SC}), defined as the Residual Hemolytic Activity (RHA), ranges from 1.0 (no depletion of hemolytic activity) to 0.0 (complete depletion of hemolytic activity). We applied the RHA metric to a set of positive and negative control nanoparticles and found that NP:C activity expressed this way is relatively consistent for

each control nanoparticle. For example, 50 mol% DOTAP nanoparticles completely depleted serum of hemolytic activity while 20 mol% DOTAP nanoparticles only depleted ~50% of hemolytic activity (Figure 2, C and Supplementary Table 1). Thus, while serum control activity may vary from day-to-day, the normalization method above results in a relatively consistent RHA value for each NP.

To validate the results of the hemolytic assay, the serum hemolytic activity and EA complement sensitivity must be confirmed. This can be achieved through inspection of the serum control data points. First, no more than 10% lysis should occur when the EA cells are incubated with buffer alone. That would eliminate background due to damaged cells. Also, each NP titration curve has a control point with EA and buffer that can be used to identify NPs that absorb light at OD_{414} as well as NPs that promote cell lysis in the absence of serum. Next, maximum lysis should approach 100%. Additional points of validation can be obtained by calculating the serum CH50, the serum dilution

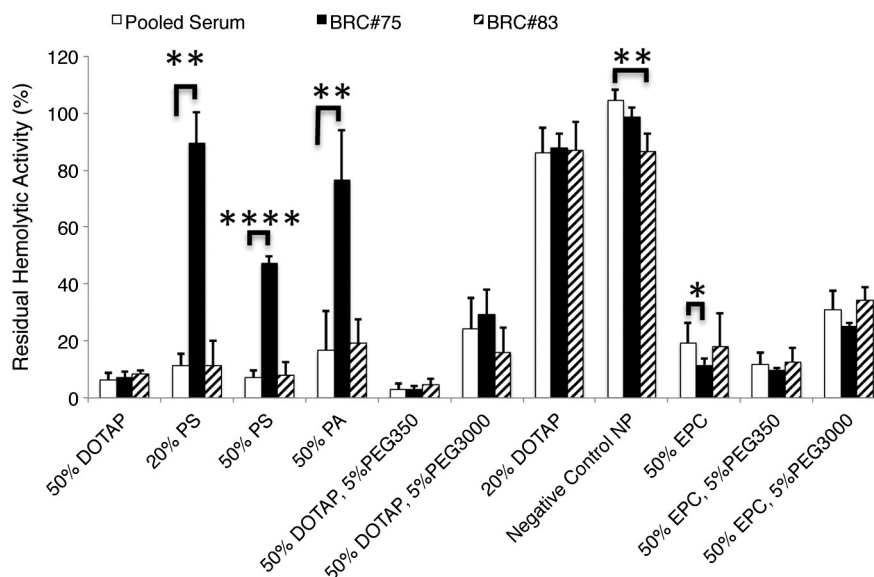


Figure 4. Variation in the NP-dependent C response. NP-dependent complement reactivity of pooled serum was compared to that of sera derived from individual donors (BRC#75 and BRC#84). Values represent mean \pm SD derived from at least 3 separate experiments. * $P < 0.05$; ** $P < 0.01$; **** $P < 0.0001$ as determined by unpaired t-test.

factor that yields 50% cell lysis (see Methods). The mean CH50 of normal serum derived from 77 successful experiments that together included 9 different EA preparations was $207 \pm \text{s.d. } 50$ U/mL. A serum control CH50 of at least 100 indicates that the EA cells are adequately sensitized and the serum is sufficiently active to successfully perform this procedure. At least one negative control particle (eliciting little or no detectable complement activity) and one positive control particle (eliciting robust C activity) were included in each experiment (Figure 2, B). Dose-dependent C activity was also observed when NPs are replaced by the complement activators zymosan, mannan, or immune complexes, confirming that all 3 pathways of complement are operative in the pooled sera (Figure 2, D).

Increase in assay sensitivity with low ionic strength buffer

The standard CH50 assay is usually conducted in an isotonic saline buffer (GVB++).²² The initial analysis of a broader range of PFOB NPs using GVB++ suggested, however, that this buffer was not sufficiently sensitive to differentiate the activity of PFOBs that only moderately activated C in vivo. For that reason we modified the hemolysis assay, employing DGVB++, a low ionic strength buffer that promotes greater C activity while retaining reaction specificity.²² To examine this point further, the C activity of a panel of nanoparticles was determined under each buffer condition. The two buffer conditions were tested in parallel experiments to ensure that testing conditions (NPs, sera and sensitized sheep cells) were uniform. Eighteen pairs of experiments were performed with each NP examined at least 5 times. As expected, NP-dependent CA was more readily detected in many cases with DGVB++ (Figure 3, A). Significant differences included positively charged particles incorporating DOTAP and negatively charged particles incorporating phosphatidylserine (PS) or the imaging agent

gadolinium- tetraazacyclododecanetetraacetic acid (Gd-DOTA). In addition, by employing DGVB++ it was possible to associate incremental NP design changes with significant differences in CA. Increases in DOTAP surface load from 2 mol% to 20 mol% ($P < 0.01$) and 20 mol% to 50 mol% ($P < 0.02$) were accompanied by stepwise increases in CA and addition of 5 mol% PEG350 or PEG3000 to particles harboring 50 mol% DOTAP was accompanied by significant decreases in CA ($P < 0.01$ and $P < 10^{-4}$, respectively). When the results obtained with the in vitro assay were compared to the in vivo findings (from Figure 1, B) a linear correlation was observed between the average RHA values derived from the in vitro assays and the average plasma C3a values derived in vivo ($R^2 = 0.80$) (Figure 3, B). While it cannot be expected that the mouse and human C systems will respond equally to all nanomaterials, it is clear that in these instances and by these criteria the two systems are in close accord.

Analysis of individual donor serum

One potential challenge in the clinical translation of NP-based therapeutics is the variation in the individual complement responses. To determine whether the hemolytic assay can detect individual variations we employed a panel of nanoparticles to compare NP:C activity of pooled serum (used up to this point to derive the above data) to that of sera derived from two healthy donors. As seen in Figure 4, the response of serum from donor BRC#83 was nearly indistinguishable from pooled serum with one notable exception being the “negative control” particle elicited a modest CA response from the BRC#83 sample but no detectable response from the pooled serum. On the other hand, serum from donor BRC#75 elicited significantly less CA from three highly negatively charged NPs [20 mol% PS, 50 mol% PS, and 50 mol% phosphatidic acid (PA)] compared with pooled

Table 1
Nonparametric tests results of the NP:C reactivity of sera derived from individuals (univariate).

Nanoparticle	Age Spearman correlation P-value	Race Kruskal Wallis P-value	Gender Wilcoxon P-value
CH50 1st series of experiments	0.6387	0.0141	0.6650
ASP8_26 (20 mol%PS)	0.5622	0.0971	0.4025
ASP8_28 (50 mol%PS)	0.4485	0.2414	0.5444
ASP9_16 (50 mol%EPC)	0.6740	0.4285	0.4705
ASP9_6 (50 mol%DOTAP)	0.6000	0.1127*	0.5444
ASP9_12 (5 mol%PEG3000)	0.7618	0.0652	0.1260*
ASP9_4 (20 mol%DOTAP)	0.5444	0.0833	0.5444
CH50 2nd series of experiments	0.5057	0.0089	0.3237
XY1-54 (Plain PFOB)	0.1498	0.1043*	0.3575
XY1-62 (50 mol%DOTAP)	0.5524	0.9898	0.9734

* indicates marginally statistically significant differences of $P \leq 0.15$.

serum and BRC#83 but was more active when tested against the positively charged particle 50 mol% EPC (Figure 4).

We next conducted a systematic comparison of the level of variation in NP:C interaction among a small group of individuals of differing race, gender and age. Sera derived from 24 healthy donors were individually tested. The average age was 36.4 years (standard deviation of 10.1 years, range of 19 to 55), 11 were male and 13 were female. By self-identified race, 14 were African American, 8 were Caucasian and 2 were Hispanic. Two NP panels were examined separately and results were analyzed together. Differences ($P \leq 0.10$) by race in RHA were found for ASP8_26 (20 mol% phosphatidylserine), ASP9_4 (20 mol% DOTAP), ASP9_12 (5 mol% PEG3000), and XY1-54 (non-functionalized PFOB) (Table 1). Lower RHA (indicative of a greater complement response) was observed in Caucasians than in African Americans for ASP8_26, ASP9_12 and XY1-54 whereas lower RHA was observed in African Americans than Caucasians for ASP9_4 (Table 2). Higher serum CH50 was also seen in the African Americans (Tables 1 and 2). There was also a trend for a gender difference for ASP9_12 with females having higher responses than males ($P = 0.1260$) (Table 1).

For each nanoparticle we compared the absolute difference in RHA between replicate experiments for a single donor to the absolute difference in RHA between donors. The absolute difference between donors was twice to three times the absolute difference between experiments for a given donor. Thus, the differences in RHA by race, gender and age for some nanoparticles were clearly attributable to demographic differences between individual donors and not due to differences (or instability) in the experimental technique. These results highlight the utility of a sensitive hemolytic assay and the importance of determining the level of individual variations in NP:C activity when the use of nanomaterials is contemplated.

Discussion

In the studies herein we extend our preliminary observations on the ability of NPs to activate C¹⁹ to examine the NP:C interactions of a wider variety of PFOBs. We show that the in vivo mouse C3a levels quantified by ELISA correlated well with human in vitro RHA measured by a modified sensitive hemolysis assay that employed the low ionic strength buffer DGVB++. In addition, the in vitro modified hemolysis assay was used to identify variations in NP:C interactions among individuals that could be of clinical significance.

The highly quantitative C3a levels generated in vivo extends the value of the mouse system in the analysis of NP-dependent C activation. Notably, the mouse system, with the extensive panel of mouse strains deficient in specific C proteins, is a relatively convenient model that facilitates the identification of the C pathways and components underlying NP:C interaction. For example, we show that the highly positively charged particle incorporating 50 mol% DOTAP, activates C in an antibody- and CP-dependent manner, with a lesser contribution by the AP and no apparent LP involvement. Unlike the in vitro C3a assay, which is hampered by high background levels caused by the accumulation of fragments generated spontaneously, the baseline C3a levels observed in vivo are relatively low, likely due to its continuous clearance in the circulation. Thus we suggest that the concurrent use of both mouse in vivo and human in vitro assays can provide more information than the use of a single system.

We also presented herein that by simply lowering the ionic strength of the buffer we were able to adapt the long-standing classic hemolytic assay procedure to accurately assess in vitro C activity using pooled or individual human sera. The procedure entails two major reactions: NPs are first pre-incubated with serum components for 30 min to permit NP-dependent CA to occur; then incremental volumes of the reaction mixture are added to antibody-sensitized sheep cells and hemolysis is monitored. This approach worked well with PFOBs, as we observed no direct interaction between NPs and EA cells in the absence of serum (and complement proteins). Although centrifugation easily separated the PFOBs from the reaction mixture, we found that the RHA obtained without and with this additional step was very similar (Supplementary Figure S6). Thus the assay may be useful to assess C activation with NPs that are not readily separated from the fluid phase of the reaction mixture.

In addition, we demonstrated significant variations in NP:C interactions in a relatively small number of sera derived from individuals of differing race, gender and age using the modified hemolysis assay. Although we did not further characterize the individual sera for these studies herein, it is likely that presence of C inhibitors, autoantibodies, and/or partial/complete C protein deficiencies, among other factors may influence the RHA. In the future the assay may be used to determine the mechanism underlying individual variations in NP:C activity.

The hemolysis assay is a procedure routinely used by hospital-based clinical laboratories and research laboratories specializing in complement-related studies. Although any laboratory could readily adapt the assay for use, one must be cognizant of certain issues. Foremost is the reactivity and

Table 2

Variations in RHA by gender and race.

	Gender						P- value	Race									P- value
	Female			Male				Black			Caucasian			Hispanic			
	n	Mean	STD	n	Mean	STD		n	Mean	STD	n	Mean	STD	n	Mean	STD	
CH50 series 1	13	301.5	96.7	11	282.7	91.6	0.6650	14	331.9	86.0	8	216.4	59.9	2	326.5	79.9	0.0141
ASP8_26 (20 mol%PS)	13	33.7	25.4	11	45.2	33.4	0.4025	14	47.9	32.5	8	22.7	19.4	2	41.9	10.9	0.0971
ASP8_28 (50 mol%PS)	13	11.6	6.3	11	15.9	11.0	0.5444	14	14.3	9.8	8	9.9	4.7	2	23.8	8.6	0.2414
ASP9_16 (50 mol%EPC)	13	6.8	3.6	11	9.2	3.4	0.4705	14	7.0	2.8	8	8.5	4.8	2	11.5	0.6	0.4285
ASP9_6 (50 mol%DOTAP)	13	4.8	3.5	11	7.5	7.5	0.5444	14	5.5	3.2	8	6.4	9.1	2	8.0	4.4	0.1127
ASP9_12 (5 mol%PEG3000)	13	71.5	29.8	11	85.5	25.7	0.1260	14	81.5	23.2	8	70.3	38.8	2	83.5	12.7	0.0652
ASP9_4 (20 mol%DOTAP)	13	45.2	23.4	11	66.5	30.3	0.5444	14	47.1	19.4	8	61.8	39.2	2	82.8	4.6	0.0833
CH50 2nd series	13	225.5	66.2	9	265.6	67.2	0.3237	13	257.3	53.7	7	207.3	90.7	2	262.5	31.8	0.0089
XY1-54 (Plain PFOB)	13	79.2	26.1	9	81.2	16.2	0.3575	13	85.6	20.2	7	66.5	23.5	2	90.7	12.4	0.1043
XY1-62 (50 mol%DOTAP)	13	7.6	3.9	9	5.3	2.7	0.9734	13	7.8	3.5	7	5.2	3.6	2	4.4	1.1	0.9898

stability of the antibody-sensitized sheep erythrocytes (EA). We have compared the assay performed with EA prepared in-house to the assay performed with EA obtained from a commercial source (CompTech). The results appear quite similar (Supplementary Table S1), suggesting that a commercially available cell preparation from a known source such as CompTech should suffice especially since in-house prepared EA may be subject to inter-laboratory disparities. Another issue relates to the use of control particles. Currently there are no commercially produced positive and negative control nanoparticles. Thus, a repository of validated control particles that are available to all interested laboratories may in the future facilitate the screening of nanomaterials for C activity.

The hemolysis assay also has intrinsic limitations. Nanoparticles that bind to complement components could artificially deplete serum of C and theoretically affect hemolytic activity without activating C. Some NPs may interfere with optical absorbance and cannot be easily separated. On the other hand, in vitro ELISA-based assays also have limitations. Some specific ELISA targets (C3a, C5a, SC5b-9, Bb) are hampered by high background signals due to spontaneous AP activation (Supplementary Figures S1, S3 and S4) while others (C4d) are not generated by all possible activation pathways (Figure 1, A). Complement activation products can also bind to nanomaterials, artificially lowering the measurable level in the fluid phase.³⁴ In addition to the above, the recognition of NP:C activity beyond the standard pathways (e.g. partial activation reactions or by-pass mechanisms) could present obstacles for any current assay. The use of multiple independent methods would serve to minimize the impact of the limitations of each of these and other assay types.

In summary, we have employed a modified in vitro hemolysis-based assay developed in conjunction with the mouse in vivo model to evaluate the complement activity of perfluorocarbon nanoparticles of varying size, charge and surface chemistry and to demonstrate significant variations in NP:C interactions in a relatively small number of sera derived from individuals of differing race, gender and age. This approach may provide the tools for an in-depth structure-activity relationship study that will guide the eventual development of biocompatible nanoparticles.

Appendix A. Supplementary data

Supplementary data to this article can be found online at <http://dx.doi.org/10.1016/j.nano.2013.10.012>.

References

- Petros RA, DeSimone JM. Strategies in the design of nanoparticles for therapeutic applications. *Nat Rev Drug Discov* 2010;**9**:615.
- Dobrovolskaia MA, McNeil SE. Immunological properties of engineered nanomaterials. *Nat Nanotechnol* 2007;**2**:469.
- Nilsson B, Korsgren O, Lambris JD, Ekdahl KN. Can cells and biomaterials in therapeutic medicine be shielded from innate immune recognition? *Trends Immunol* 2010;**31**:32.
- Ricklin D, Hajishengallis G, Yang K, Lambris JD. Complement: a key system for immune surveillance and homeostasis. *Nat Immunol* 2010;**11**:785.
- Chanan-Khan A, et al. Complement activation following first exposure to pegylated liposomal doxorubicin (Doxil): possible role in hypersensitivity reactions. *Ann Oncol* 2003;**14**:1430.
- Szebeni J, Muggia F, Gabizon A, Barenholz Y. Activation of complement by therapeutic liposomes and other lipid excipient-based therapeutic products: prediction and prevention. *Adv Drug Deliv Rev* 2011;**63**:1020.
- Szebeni J. Complement activation-related pseudoallergy: a new class of drug-induced acute immune toxicity. *Toxicology* 2005;**216**:106.
- Volanakis JE. In: Volanakis JE, Frank MM, editors. *The human complement system in health and disease*. New York: Marcel Dekker, Inc; 1998. p. 9-32.
- Liszewski MK, Atkinson JP. In: Volanakis JE, Frank MM, editors. *The human complement system in health and disease*. New York: Marcel Dekker; 1998. p. 149-66.
- Lanza GM, et al. A novel site-targeted ultrasonic contrast agent with broad biomedical application. *Circulation* 1996;**94**:3334.
- Lanza GM, et al. Molecular imaging of stretch-induced tissue factor expression in carotid arteries with intravascular ultrasound. *Invest Radiol* 2000;**35**:227.
- Flacke S, et al. Novel MRI contrast agent for molecular imaging of fibrin: implications for detecting vulnerable plaques. *Circulation* 2001;**104**:1280.
- Lanza GM, et al. Targeted antiproliferative drug delivery to vascular smooth muscle cells with a magnetic resonance imaging nanoparticle contrast agent: implications for rational therapy of restenosis. *Circulation* 2002;**106**:2842.
- Lanza GM, et al. Theragnostics for tumor and plaque angiogenesis with perfluorocarbon nanoemulsions. *Angiogenesis* 2010;**13**:189.

15. Schmieder AH, et al. Characterization of early neovascular response to acute lung ischemia using simultaneous F/ H MR molecular imaging. *Angiogenesis* 2013(Aug 6).
16. Cyrus T, Wickline SA, Lanza GM. Nanotechnology in interventional cardiology. Wiley interdisciplinary reviews. *Nanomed Nanobiotechnol* 2012;**4**:82.
17. Zhou HF, et al. Suppression of inflammation in a mouse model of rheumatoid arthritis using targeted lipase-labile fumagillin prodrug nanoparticles. *Biomaterials* 2012;**33**:8632.
18. Schmieder AH, et al. Molecular MR imaging of neovascular progression in the Vx2 tumor with alphavbeta3-targeted paramagnetic nanoparticles. *Radiology* 2013;**268**:470.
19. Pham CT, et al. Variable antibody-dependent activation of complement by functionalized phospholipid nanoparticle surfaces. *J Biol Chem* Jan 7, 2011;**286**:123.
20. Fischer MB, et al. Regulation of the B cell response to T-dependent antigens by classical pathway complement. *J Immunol* 1996;**157**:549.
21. Matsumoto M, et al. Abrogation of the alternative complement pathway by targeted deletion of murine factor B. *Proc Natl Acad Sci U S A* 1997;**94**:8720.
22. Whaley K. In: Whaley K, editor. *Methods in complement for clinical immunologists*. New York: Churchill Livingstone; 1985. p. 77-139.
23. Morgan BP. In: Morgan BP, editor. *Methods in Molecular Biology: Complement Methods and Protocols*. Humana Press: Totawa, New Jersey; 2000. p. 61-71.
24. McGill R, Tukey JW, Larsen WA. Variations of box plots. *Am Stat* 1978;**32**:12.
25. Thurman JM, Holers VM. The central role of the alternative complement pathway in human disease. *J Immunol* 2006;**176**:1305.
26. Holers VM. The spectrum of complement alternative pathway-mediated diseases. *Immunol Rev* 2008;**223**:300.
27. Malhotra R, et al. Glycosylation changes of IgG associated with rheumatoid arthritis can activate complement via the mannose-binding protein. *Nat Med* 1995;**1**:237.
28. Zhang M, et al. Activation of the lectin pathway by natural IgM in a model of ischemia/reperfusion injury. *J Immunol* 2006;**177**:4727.
29. Hamad I, et al. Complement activation by PEGylated single-walled carbon nanotubes is independent of C1q and alternative pathway turnover. *Mol Immunol* 2008;**45**:3797.
30. Hamad I, Hunter AC, Szebeni J, Moghimi SM. Poly(ethylene glycol)s generate complement activation products in human serum through increased alternative pathway turnover and a MASP-2-dependent process. *Mol Immunol* 2008;**46**:225.
31. Hamad I, et al. Distinct polymer architecture mediates switching of complement activation pathways at the nanosphere-serum interface: implications for stealth nanoparticle engineering. *ACS Nano* 2010;**4**:6629.
32. Salvador-Morales C, Zhang L, Langer R, Farokhzad OC. Immunocompatibility properties of lipid-polymer hybrid nanoparticles with heterogeneous surface functional groups. *Biomaterials* 2009;**30**:2231.
33. Meerasa A, Huang JG, Gu FX. CH(50): a revisited hemolytic complement consumption assay for evaluation of nanoparticles and blood plasma protein interaction. *Curr Drug Deliv* 2011;**8**:290.
34. Cheung AK, Parker CJ, Wilcox LA, Janatova J. Activation of complement by hemodialysis membranes: polyacrylonitrile binds more C3a than cuprophane. *Kidney Int* 1990;**37**:1055.